PAPER • OPEN ACCESS

Theoretical accuracy assessment of model-based photogrammetric approach for pose estimation of cylindrical elements

To cite this article: Gorka Kortaberria *et al* 2019 *Meas. Sci. Technol.* **30** 055003

View the article online for updates and enhancements.

Theoretical accuracy assessment of model-based photogrammetric approach for pose estimation of cylindrical elements

Gorka Kortaberria[1,4] [ORCID]**, Eneko Gomez-Acedo**[1]**, Jorge Molina**[2]**, Alberto Tellaeche**[2] **and Rikardo Minguez**[3]

[1] Department of Mechanical Engineering, IK4-Tekniker, Eibar 20600, Spain
[2] Department of Smart and Autonomous Systems, IK4-Tekniker, Eibar 20600, Spain
[3] Department of Graphic Design and Engineering Projects, University of the Basque Country, Bilbao 48013, Spain

E-mail: eneko.gomez-acedo@tekniker.es (EG-A), jorge.molina@tekniker.es (JM), alberto.tellaeche@tekniker.es (AT), rikardo.minguez@ehu.eus and gorka.kortaberria@tekniker.es

CrossMark

Abstract

In this research, a multi-view photogrammetric model was developed and tested in simulation in order to understand its capabilities for close-range photogrammetric applications. It was based on contour line detection and least squares geometrical fitting of a cylindrical geometry from multiple views. To feed and validate this model, synthetic data were created for several cylinders poses and camera network set-up. The simulation chain comprises three main stages: synthetic image creation, image data processing by means of shape-matching and cylinder pose estimation based on developed photogrammetric model. Beforehand, *a priori* data was theoretically established according to a common reference for both for intrinsic and extrinsic parameters of the cameras. The preliminary results highlight that the model is suitable for close-range photogrammetry and sensible to *a priori* known data as well as to image data quality. These results were compared against other validated geometrical methods to assure that the model is truthful. Preliminary results show that the accuracy of the model ranges between 1/1000 and 1/20 000 for multiple poses and cylinder dimensions. Moreover the simulation procedure has been enhanced with a Montecarlo approach to estimate more realistic pose uncertainties considering possible imaging error sources.

Keywords: model-based, simulation, cylinder pose, photogrammetry, contour lines, least square fitting, uncertainty

(Some figures may appear in colour only in the online journal)

1. Introduction

1.1. The context and limitations

The recovery of the 3D geometric information from 2D images is a fundamental problem in computer vision and photogrammetry fields. Recent reviews and advances in this field regarding this problem are presented in Luhmann *et al* (2013, 2006, 2016), Crc (2015) and Heipke *et al* (2016). Most

of the approaches among multiple perspectives and features are based on collinearity equations and on a correspondence problem. Although these strategies are valid for most cases, sometimes they are not feasible. One of the main limitations of these methods is the preparation of the scene when the geometric elements to be measured are either large (>5 m), far away (>20 m) or hardly accessible. Harsh environments, such as those where elements to be measured are thermal emitting surfaces, are also challenging for traditional solutions as the location of artificial targets on the surface is not possible.

---

[4] Author to whom any correspondence should be addressed.

Occlusion problems for multi-view approaches is another limiting factor for target-based photogrammetry where line of sight is not guaranteed. Moreover, the measurement in solar plants environment suffer from poor object illumination and signalization problems as well as possible image recording difficulties due to air convection of hot surfaces. To tackle these drawbacks, model-based approaches are advisable in order to avoid scene preparation and to estimate the pose of the element of interest by means of geometric fitting. These kind of solutions are based on high quality detection of contour points that define the element or elements to be measured. Depending on this, high accuracies for 3D element verification, pose estimation or tracking can be obtained when the camera network employed assures image ray suitable convergence. One of the limitations corresponds to necessary approximated values of the element to be measured and previous camera network calibration solving (Fraser 2013, Fraser and Stamatopoulos 2014, Summan *et al* 2015, Luhmann *et al* 2016). The method can be used for several geometric components spatial determination such as lines, cylinders and circles.

1.2. Background

Pose estimation of geometric elements is a common requirement in 2D and 3D vision based applications, where different methods have been developed and studied to tackle this problem from different point of views. In the bibliography different methods (see figure 1) can be found such as pose orientation from known points (Oberkampf *et al* 1996, Triggs 1999, Zhi and Tang 2002, Xu and Liu 2013), pose estimation using shape-based 3D matching (Osada *et al* 2001, Rosenhahn *et al* 2006, Teck *et al* 2010, Yang *et al* 2016), pose estimation using surface-based 3D matching (Rabbani and Van Den Heuvel 2005, Su and Bethel 2010, Liu *et al* 2013, Paláncz *et al* 2016, Figueiredo *et al* 2017) and pose estimation based on model-based approaches. Pose estimation is required in motion applications as well as for measuring, bin-picking or even alignment tasks. The selection of the most suitable approach needs to consider multiple factors directly related to required measuring specifications. In this research the model-based approach has been selected as the accuracy, large working distance, round surface form, harsh measuring environment and high number of measuring perspectives are demanding requirements which other approaches do not fit.

This paper presents not only a novel photogrammetric simulation approach, but also a theoretical simulation chain to design a camera network that fulfills and enables one to guarantee that the measuring accuracy of the employed approach is under the application tolerance.

Thus, both aspects were analyzed by previous researches in order to provide a general overview in this field and to know more about the approaches followed in each case, as well as about the obtained results.

In order to evaluate if a photogrammetric procedures is fit to purpose, simulation based approaches permitting modelling testing and output result reliable quantification are required. Usually known as camera network design problem, this topic has been deeply studied in the following two main

approaches, one of them uses mathematical models (Dunn 2007, Alsadik *et al* 2012, Dall'Asta *et al* 2015, El-hamrawy *et al* 2016, Tushev and Sukhovilov 2017) and the other uses synthetic data, following the 'design by simulation' concept (Olague and Mohr 2002, Becker *et al* 2011, Piatti and Lerma 2013).

Focused on the second method, which is similar to the simulation procedure described in this paper, Piatti and Lerma (2013) developed a virtual simulator that underpins the design of a photogrammetric measurement based on 3D scenes (Becker *et al* 2011) presents a free ray tracing software to build up a virtual close range photogrammetric sensor and simulate 3D scenes based on this simulation approach, and finally (Buffa *et al* 2016) presents a simulation study for a dimensional characterization of an antenna combining different tools.

Regarding simulation packages (software, libraries) for a photogrammetric network design and optimization based on nominal or synthetic data (images or geometrical information), there are few available options. The main ones are the combination of Spatial Analyzer© and VSTARS© inspection tools, academic softwares such as Phox© (Luhmann 2016) for photogrammetric design and parametric mathematical understanding, photogrammetric libraries integrated in computer vision Matlab© toolbox (Tushev and Sukhovilov 2017), opensource libraries (MICMAC©, APERO©, SFM©, GRAPHOS©) for dense point cloud reconstruction, etc.

The above-mentioned simulation alternatives and industrial photogrammetric solutions enable one to measure not only the spatial position of artificial targets or fixtures, but also the location of some natural features such as holes, lines (Gruen and Li 1991), pipes (Veldhuis and Vosselman 1998, Zhang *et al* 2017) or spheres in 3D. However, together with this objective, these alternatives need to triangulate these features from multiple perspectives with determined incidence angles. Therefore, the accuracy is reduced most cases and the correspondence problem must then be solved. A common approach is to use epipolar geometry to enhance stereo image matching strategies.

Previously mentioned approaches do not take into consideration the cases where the photogrammetric problem is solved by means of a minimization of the distance among image rays and the spatial geometric element to be fitted and measured. They offer the possibility to estimate the pose of a geometric element adjusting the 3D coordinates of the targets that define the object. Therefore, there is a lack of knowledge in this sense when this kind of ray projection based photogrammetric approaches are required. A general overview of this tracking 3D methods is described in Doignon (2007), where limitations and challenges are also mentioned.

In the literature, there are few references regarding photogrammetric approaches where the correspondence problem (Hilton 2005, Fraser *et al* 2010) is avoided. Most of the existing references are theoretical studies about the modelling and the problems derived from the geometrical determination of 3D elements such as lines, circles or cylinders. A survey and estimation approaches for these geometric elements is presented in Doignon (2007). However, compared to these
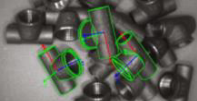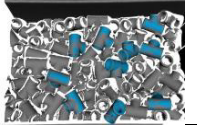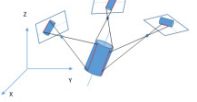
Pose estimation approaches	Scheme	Data type to be analyzed
Spatial resection with known points		2D image data (known targets)
Shape-based 3D matching		2D image data (shape)
Surface-based 3D matching		3D point cloud (segmentation and fitting)
Model-based		2D image data (contour points)

Figure 1. Review of cylinder pose estimation methods.

geometries, the literature regarding the pose estimation of cylindrical objects with constant radius, is somewhat sparse.

Moreover, although other geometrical features have been studied more in detail, there are two main classifications for the references based on single-view or multi-view approaches for cylinder pose estimation. In any of this cases, the obtained relative accuracy is not studied for large scale applications.

Both for single view (Shiu and Huang 1991b, Ferri *et al* 1993, Puech *et al* 1997, Penman and Alwesh 2006, Doignon and De Mathelin 2007, Liu and Hu 2014) approaches or multi-view ones (Houqin and Jianbo 2008, Becke 2015, Teney and Piater 2014, Becke and Schlegl 2015, Zhu *et al* 2015, Zhang *et al* 2017), cylinder pose estimation can be estimated based on several approaches or on a combination of them. Depending on the image data taken into consideration, only cylinder orientation in three degrees of freedom (dof) or five dof pose can be established employing the contour data corresponding to cylinder's circular borders. The combination of different contour data can tackle a more robust pose estimation combining both, orientation and position results.

On the one hand, there are different approaches for monocular camera methods such as probabilistic ones (Hanekr *et al* 1999), basic or more complex models depending on the dof number for the cylinder's pose (Huang *et al* 1996, Doignon and De Mathelin 2007), models considering different image data from shape matching outputs (Shiu and Huang 1991a) or cases where the geometrical dimensions of the element are known *a priori* (Huang *et al* 1996, Puech *et al* 1997, Renaud *et al* 2005, Liu and Hu 2014).

Apart from this, 3d circle pose estimation is solved in Shiu and Huang (1991a) and Andresen and Yu (1994) for the same approach where even the orientation is established by ellipse modelling and fitting approach.

On the other hand, there are multiple view approaches considering more complex and robust camera networks both for cylinder pose and 3D line detection.

For example, a canonical representation based software is presented in Navab and Appel (2006) for stereo or multi-views, theoretical preliminary modelling for pose estimation based on contour data and single or multi-view approaches in Becke (2015), semi-automatic linear feature extraction algorithm for estimation of 3D elements from multi-view approaches based on LSB-Snakes in Gruen and Li (1991), the reconstruction of straight and curved pipes from digital images with not corresponding points in Veldhuis and Vosselman (1998) and Zhang *et al* (2017), a least-squares method for locating a linear object by using its multiple parallel projections, etc…

As a summary of this literature compilation and analysis, the following list indicates the main difficulties and drawbacks that must be studied in detail so as to overcome them:

- In most cases, image noise is not taken into account in the simulation which is advisable for reliable model characterization
- The models are not applied for large-scale applications or case studies where the errors are amplified due to projection effects.
- Measuring solution validation against validated sources or tools is missing.
- Suitable feature point extraction is not usually available.
- Tools for accurate synthetic data creation (geometrical or image data) are not available.

1.3. The application

The research tends to enable an accuracy and robustness simulation of a model-based photogrammetric approach for a cylinder pose estimation when the element to be measured is hardly measurable with artificial targets (Knyaz 1998, Joon Ahn and Rauh 2001, Shortis *et al* 2004, Wijenayake *et al* 2014, Guo *et al* 2016). Thus, our approach to cylinder pose robust estimation differs from traditional approaches which
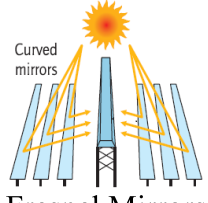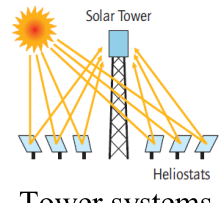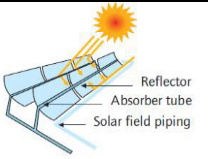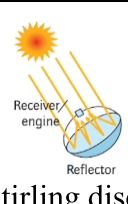
Concentrator type	Lineal	Punctual	
Discrete	Fresnel Mirrors	Tower systems	Fixed focus *(Evacuates the heat easily)*
Continuous	Cylindrical parabolic mirrors	Stirling discs	Mobile focus *(Receives more energy)*

Figure 2. Review of concentration solar power (CSP) technology.

avoid the correspondence problem among images and multiple view perspectives.

The application is focused on thermal concentration applications, (see figure 2) where positioning a closed loop of the moving receivers is required for high energy efficiency performances. Traditional photogrammetric approaches (Shortis and Johnston 1996, Pappa *et al* 2001, Pottler *et al* 2005, Shortis *et al* 2008, Stynes and Ihas 2012, King *et al* 2013, Hafez *et al* 2017) are not suitable because of surface curvature and the impossibility to add distributed targets over the element due to high working temperatures and solar flux concentrations. Another disadvantage of traditional photogrammetric approaches is related to the high incidence angles that are required for planar targets in curved surface introducing target center measurement inaccuracies. In addition, the approach described in this article aims to develop more flexible photogrammetric solutions for 3D scenes than those offered by commercial solutions. Moreover, model-based methods are not integrated in these industrial software, which means that, in order to quantify the scope and design the best suitable measuring network considering the real scene requirements, it is necessary to carry out this modelling and test its performance.

1.4. Main objectives of the research

The objectives of the research are to develop, implement and validate a model-based photogrammetric simulation tool in order to assess the six dof positioning accuracy of a cylinder for a specific camera network and synthetic image data. Is it not an optimization procedure but a test and accuracy assessment approach for design purposes of this photogrammetric method. Therefore, the main error sources are studied, and the most suitable camera network is designed and stablished by means of developed simulation tools. The results of the research will enable one to quantify and determine the accuracy and suitability of this photogrammetric approach for large parts and working distances in harsh environments. Model testing will also describe the limitations for this

photogrammetric approach offering the possibility to assess the cons and pros against traditional approaches.

2. Materials and methods

2.1. Description of the simulation method

The overall method comprises several tools, an implementation of a model (cost function), which enables the estimation of the five dof positioning of a cylinder based on contour points and a Montecarlo approachfor uncertainty assessment. The rotation of the cylinder around its axis is not controlled by the model. This model is fed with image data points extracted from synthetic images. The camera network (extrinsic orientation), the 3D scene and imaging parameters are established and the synthetic images are generated for each cylinder's spatial pose. For each cylinder pose, three images are generated for three camera views. These images are depict grey values ranging from 0 to 255 values simulating a 3507×2480 pixel camera and 6 mm principal distance lens. The pixel size is 2.8387 μm which is the scaling factor to convert pixel points to metric image points in mm. Afterwards, these images are processed with an image processing algorithm and data contour data points are obtained for each camera and pose with sub-pixel edge extraction methods. Eventually, these data points, camera network and an *a priori* geometry describing the 3D scene are imported in the photogrammetric model implemented in an engineering simulation environment. The model estimates for each image combination and fixed camera network, the real pose of the cylinder, minimizing the tangential distances among the light rays projected from image planes to the 3D geometry.

In order to obtain more realistic output results, the model has been improved with a Montecarlo simulation approach. Once the contour points are extracted from images, these pixel points are modified by random distribution error sources to evaluate their effect on the model's output. This process is repeated n times and the model output result is stored for statistical distribution analysis. The overall simulation workflow is presented below (see figure 3).
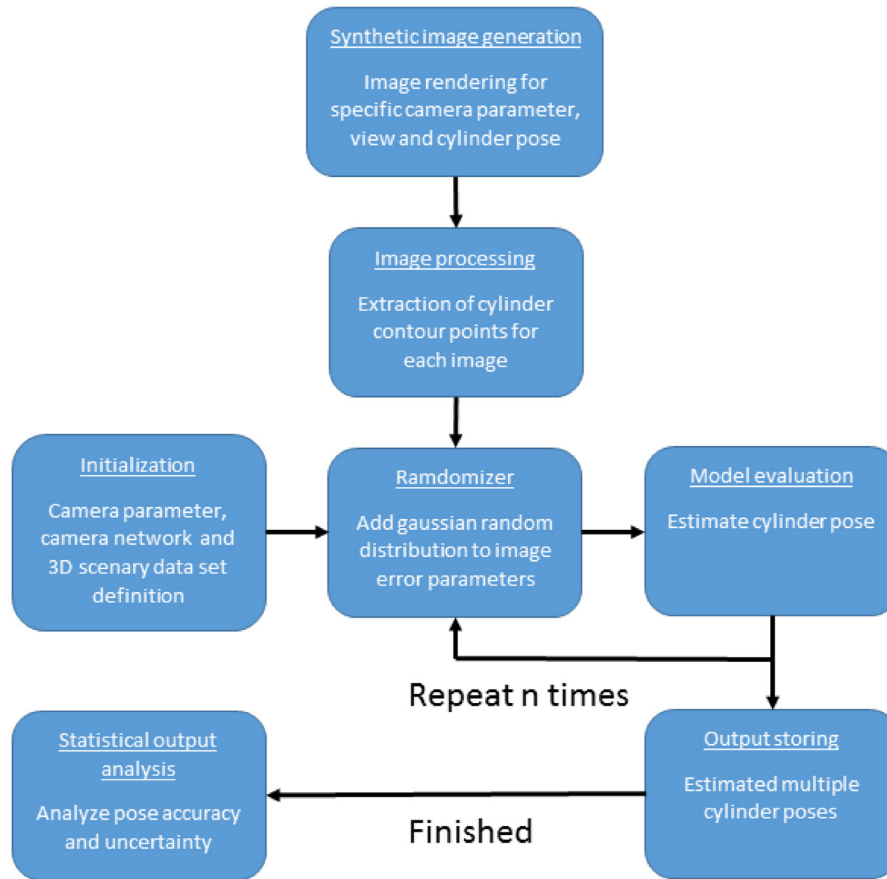
Figure 3. Simulation consecutive stages and overall process workflow.
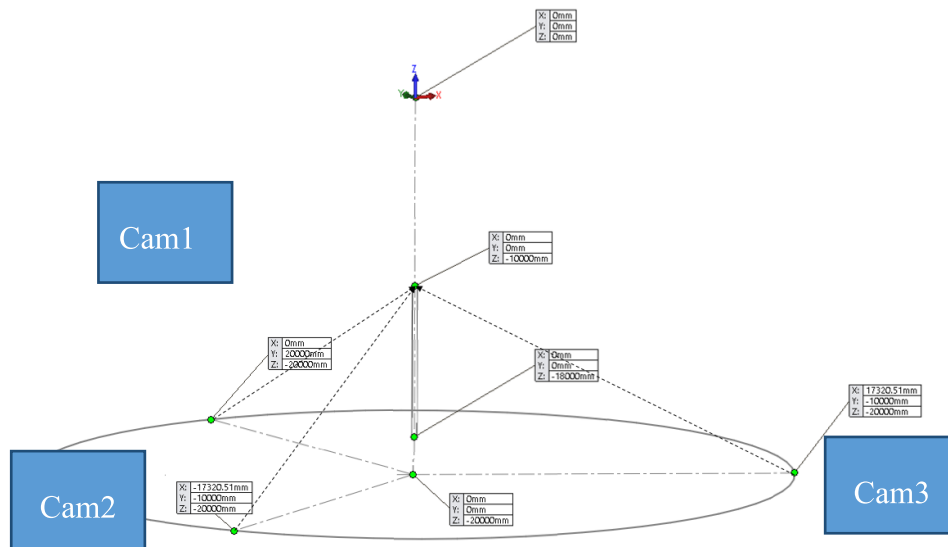
Figure 4. Cylinder vertical pose definition and camera network (extrinsic orientation) establishment.

2.2. Implementation and modelling

2.2.1. Synthetic data generation. In order to generate synthetic images, first of all the 3D scene is created 20 m away in radius from camera positions (see figure 4). In this case, 3D geometry comprises a cylinder of 8 m length and 250 mm diameter. This element is positioned and oriented according to

a reference system simulating difference poses. For instance, vertical orientation and centered position (Pose1) or totally oblique ones (Poses 2 and 3). After the several poses are established, the camera views are added for the same reference system. These views (three cameras) are fixed and require identifying several parameters, such as the position, the pointing orientation, the principal distance and image sensor

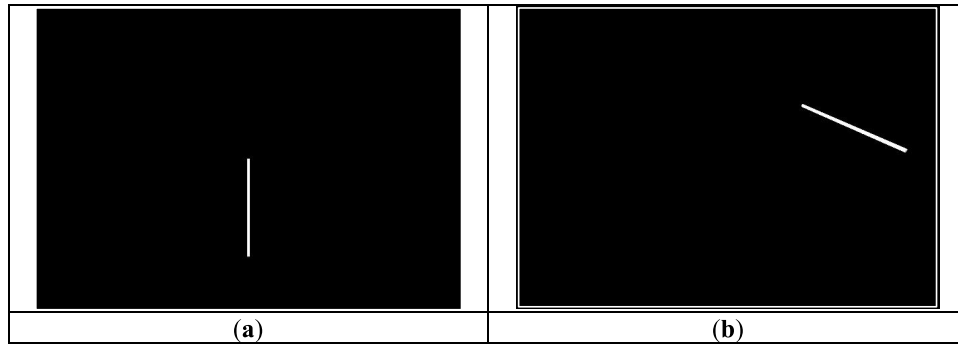**Figure 5.** Synthetic images for cylinder's several poses from the same camera field of view (see camera 1 from figure 1. (a) Vertical pose of the cylinder. (b) Oblique pose of the cylinder.

dimensions. The field of view depends on the principal distance, lens aperture, selected camera model and therefore in sensors dimensions. Real illumination aspects affecting image generation as well as optical lens distortion are not considered in this step as the design environment is not prepared for this aim. However, imaging imperfections will be considered in Monte-carlo simulation process as image noise error sources.

In the real application, object signalization limitations as well as image distortion effects will appear and directly affect the image data quality and therefore the performance of the model. While image distortion errors can be modelled, characterized by offline or self intrinsic calibration approaches (Fraser 2013, Luhmann *et al* 2016) and compensated as it is a systematic optical error source, object detection and contour point data extraction is a demanding requirement in high solar flux concentration applications (Lee *et al* 2013, Ruelas *et al* 2017). In order to minimize imaging errors and optimize image acquisition and processing steps, implemented cameras are expected to work in the infrared spectrum with dynamic range fitting which higlights the contrast between cylinder contour points and the background. In this manner, the shape-based matching process is simplified and optimized as the images contain less and more useful information speeding up image processing tasks.

Returning back to the image generation tool, once geometric parameters are settled (see figure 5), different cameras can be selected, and synthetic images are rendered (full grey level) and generated.

2.2.2. Image data processing. The employed image processing approach is based on shape matching methods that enable the finding and location of the objects of interest in an image. Within this aim, a suitable image pattern is required to define objects that are represented and recognized by their shape. There are multiple ways to determine or describe the shape of an object. In this paper, the shape is extracted by selecting all those points whose gradient exceeds a certain threshold. Typically, the points correspond to the contours of the object. The main image processing steps for previously generated synthetic images are described in the following workflow:

1. Image importation
2. Image pre-processing: a binarization on a greyscale image is applied to obtain a black and white image establishing a suitable threshold.
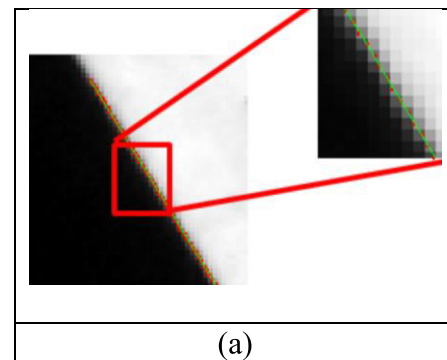

Figure 6. Sub-pixel edge location (red points) and line fitting (in green).

3. Shape based-matching (Harun and Sulaiman 2011): this is the most challenging phase of the overall image processing procedure because following tasks depend on its output. The shape based- matching algorithm tries to find the corresponding shape of an element comparing the image data against a trained pattern.. It does not use the gray values of pixels and their neighborhood as template but describes the model by the shapes of contours. This process is divided in two main steps. First of all, the shape-based pattern is defined in a sample image and trained to become the image pattern as robust as possible considering effects such as neighborhood points, contrast, noise, occlusions or even perspective changes (rotation, scale variation, etc). Secondly, this trained pattern is applied as an operator in an image where the object to be detected appears and the object and its region of interest (ROI) are determined correspondingly.

4. Edge data point extraction: Once the ROI of the object is restricted, edge extraction operators are applied to define the contour points of the shape (see figure 6). In order to speed up the subpixel-precise edge extraction, it is recommendable to apply it only to a reduced ROI. As accuracy is required for the vision based application, sub-pixel edge extraction operators are used (see figure 5). The main steps for image data extraction are: creation of sub-pixel contours by means of edge operators such as *threshold_sub_pix* and selection of relevant points where some of the segments are deleted, and others are combined to define the edge of interest. Usually a primitive
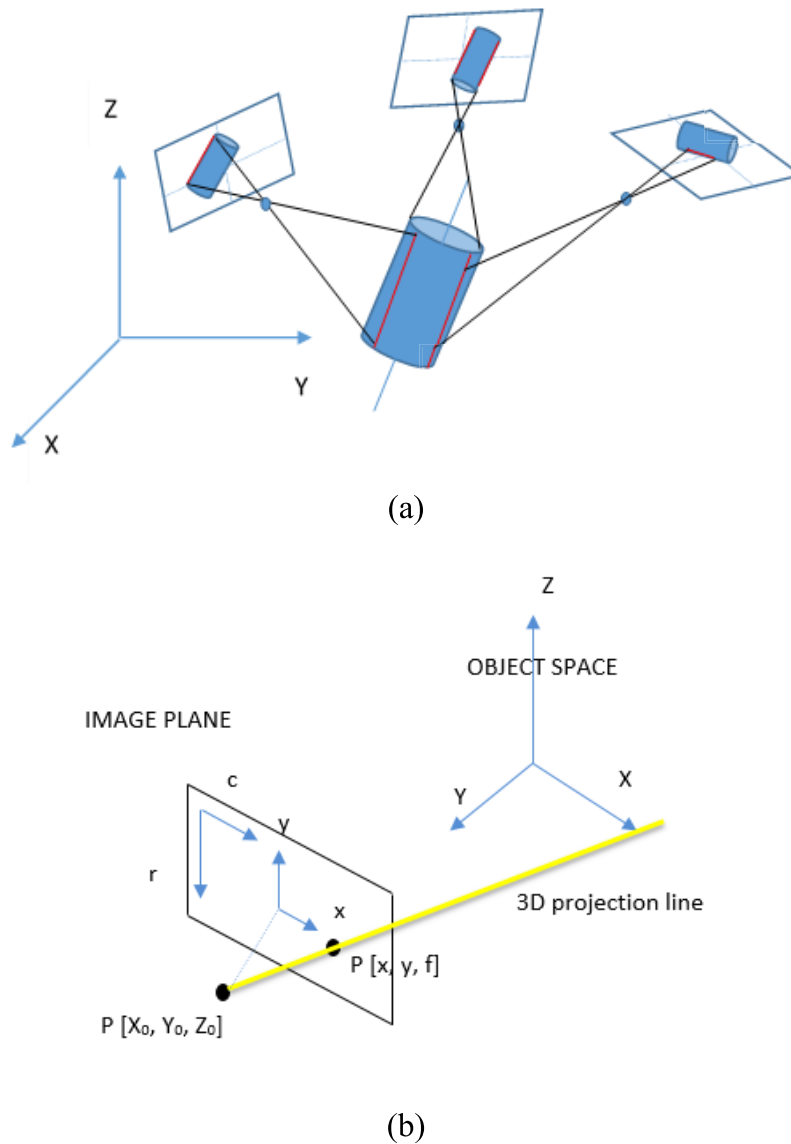
(a)

(b)

Figure 7. Edge method for cylinder pose estimation. (a) Multi-view 3D representation of the model (b) projection model from image plane to 3D space.

fitting step follows these previous steps, but in this case, is not necessary.

5. File creation for each image with contour point: finally, an Ascii file is created with these data for each image where the points corresponding to the contour points are described in row and columns in pixels units. These points do not consider image noise nor imaging parameter uncertainties.

2.2.3. Modelling. The core of this research is a photogrammetric model based on light ray projection from image planes to 3D space. Each image point and the projection center of each camera define a light ray that is tangent to the cylinder whose pose is to be found. Establishing the distances among the light rays and the geometric element and minimizing them enables to estimate the element's parameters.

The proposed methodology is not based on traditional approaches that employ artificial targets to measure a specific geometry. Usually, the 3D positions of these targets are obtained and then a least square algorithm is applied to estimate the most approximated element that fits with these 3D points. This common approach requires to assure the correspondence of the points enabling their triangulation, but this requirement is not always reached. When the element to be measured is, for example, a cylinder, the aforementioned approach is not the most suitable one. Thus, another approach is necessary to solve this limitation. The developed model for estimating the five dof positioning of a cylinder comprises an alternative approach based on Best-fit adjustment of a cylinder to measured 2D contour points in multiple images (see figure 7).

On the one hand, the inputs that feed this model are the contour points of each image, a camera network definition around those points, image parameters (principal distance and image scaling factor), image dimensions (pixel number) and an *a priori* cylinder pose (position, orientation) as well as dimensions (radius). On other hand, the output values are the real position and orientation (pose) of the cylinder related
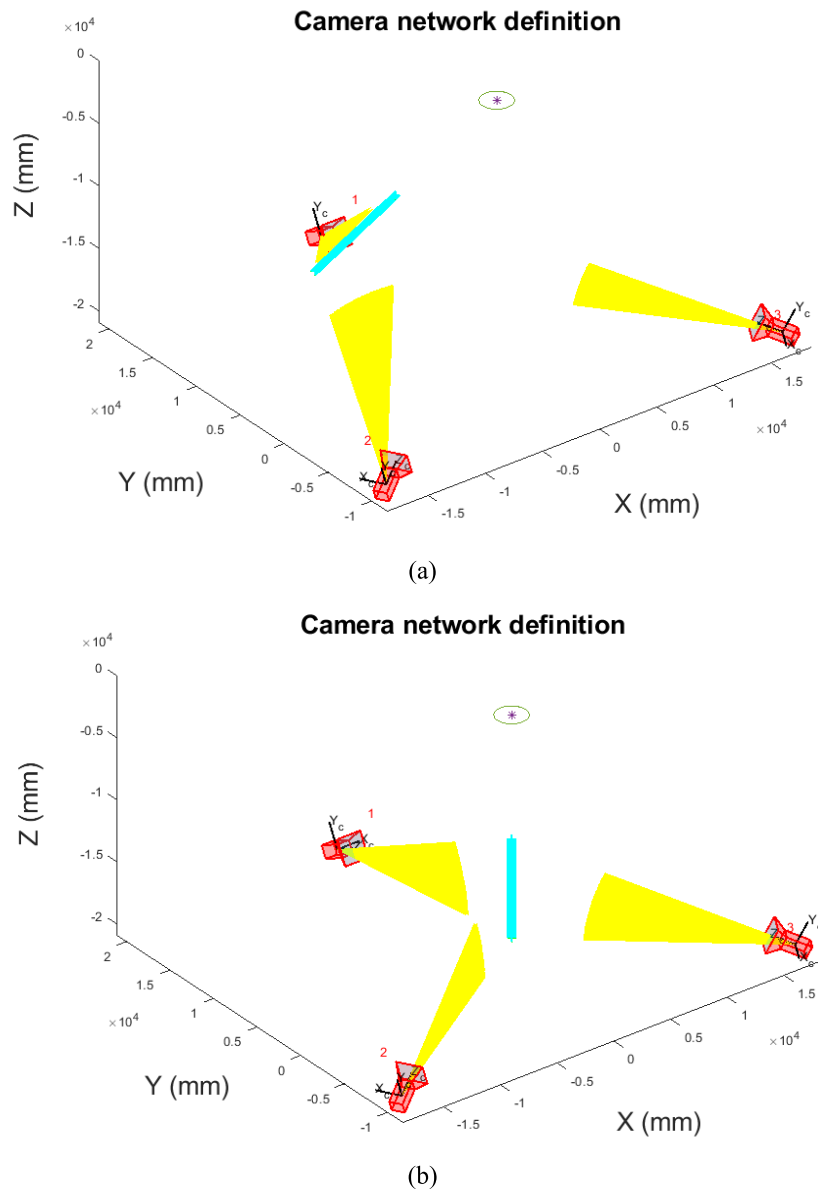
(a)

(b)

Figure 8. Photogrammetric model representation for several cylinder poses (in blue) and light rays (in yellow) pointing towards the primitive. (a) Oblique pose. (b) Vertical pose.

to a fixed coordinate system. Indeed, the pose of the cylinder is defined as 2 points P1 and P2 corresponding to the axis (see figure 10) for enabling an easier simulation result interpretation.

Model's performance is studied by means of inverse problem approaches which minimize the tangential distances among the light rays and the cylinder to be calculated. These rays are created for each image considering each image point ($Z = 0$) and the projection center (same for each image). The light rays are fitted to 3D lines that are defined in a common reference system shown in figure 3. In order to estimate the tangential distances for each ray and image, a 3D intersection function is employed. This function considers the estimation of the distances between each image ray (3D line) and cylinder axis and accordingly, estimating the tangential distances (see figure 8). The cylinder's pose is obtained by minimizing iteratively these distances.

In the following lines, a detailed mathematical description of the model is presented and the data flow is explained.

The starting point for the model are the image data of the contour points extracted from the synthetic images. For a specific cylinder pose, three files with image data are imported to the developed model. Each file corresponds to a camera and an interextrinsic orientation of this camera regarding to the absolute reference system.Besides, approximate values of the cylinder pose are required as input data.

This data in pixels (*rc*) is transformed and scaled (*m*) to metric data (mm) taking into account image's horizontal and verticals dimensions (dimHor and dimVert) and a rotation ($\alpha = 90°$) between coordinate systems. The data *xy* is in camera local coordinates. The applied plane transformation is,

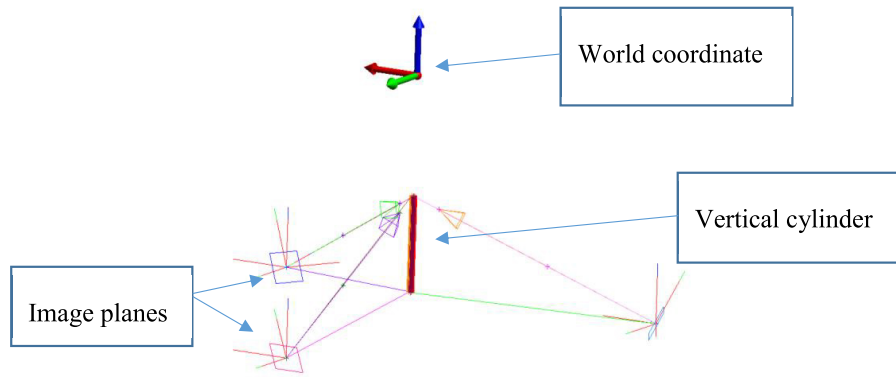$$x = m \cdot (R \cdot rc + T) \tag{1}$$

Figure 9. Definition of validation 3D pose and reference data processing with SA tool.

$$\begin{bmatrix} x \\ y \end{bmatrix} = m \cdot \left(\begin{bmatrix} \cos\alpha & -\sin\alpha \\ \sin\alpha & \cos\alpha \end{bmatrix} \cdot \begin{bmatrix} r \\ c \end{bmatrix} + \begin{bmatrix} \text{dimHor}/2 \\ \text{dimVert}/2 \end{bmatrix} \right) \cdot \quad (2)$$

Once each contour point is transformed for each image plane, a third coordinate is added to *xy* with the value of the focal distance (*f*). Thus, for each image point $x'y'z'$ coordinates are available in local coordinates.

$$\begin{bmatrix} x' \\ y' \\ z' \end{bmatrix} = \begin{bmatrix} x \\ y \\ f \end{bmatrix}. \quad (3)$$

After this transformation, another spatial transformation is required for each point to convert the $x'y'z'$ local coordinates to spatial *XYZ* coordinates corresponding to the main reference system. *R* (rotation matrix) and X_0 (translation vector) parameters define the extrinsic orientation and translation of the image plane (projection center) regarding to absolute reference system. These parameters are supposed to be known from previous calibration step.

$$X = X_0 + R^{-1} \cdot x' \quad (4)$$

$$\begin{bmatrix} X \\ Y \\ Z \end{bmatrix} = \begin{bmatrix} X_0 \\ Y_0 \\ Z_0 \end{bmatrix} + \begin{bmatrix} r_{11} & r_{21} & r_{31} \\ r_{12} & r_{22} & r_{32} \\ r_{13} & r_{23} & r_{33} \end{bmatrix} \cdot \begin{bmatrix} x' \\ y' \\ z' \end{bmatrix}. \quad (5)$$

With each transformed image point $(X_iY_iZ_i)$ and the projection center point $(X_0Y_0Z_0)$ of its corresponding camera, 3D lines are created (see figure 6). A straight line (X_{li}) between each transformed image point P_i (X_i, Y_i, Z_i) and P_0 (X_0, Y_0, Z_0) in parametric form is defined by:

$$X_{li} = X_i + t \cdot (X_0 - X_i) \quad (6)$$

$$\begin{bmatrix} X_{li} \\ Y_{li} \\ Z_{li} \end{bmatrix} = \begin{bmatrix} X_i \\ Y_i \\ Z_i \end{bmatrix} + t \cdot \begin{bmatrix} X_0 - X_i \\ Y_0 - Y_i \\ Z_0 Z_i \end{bmatrix} = \begin{bmatrix} X_i \\ Y_i \\ Z_i \end{bmatrix} + t \cdot \begin{bmatrix} a \\ b \\ c \end{bmatrix}. \quad (7)$$

Here P_i (X_i, Y_i, Z_i) is any image point corresponding to the line and the direction cosines are
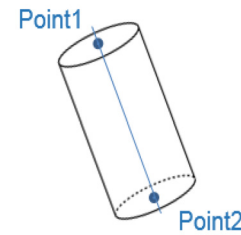
$$\frac{X_0 - X_i}{d} = a \quad (8)$$

Figure 10. Cylinder pose definition based on two spatial points (P1, P2).

$$\frac{Y_0 - Y_i}{d} = b \quad (9)$$

$$\frac{Z_0 - Z_i}{d} = c. \quad (10)$$

Where $d = \sqrt{(X_0 - X_i)^2 + (Y_0 - Y_i)^2 + (Z_0 - Z_i)^2}.$ (11)

The following step is to estimate the intersection point between each line (X_{li}) and the approximated axis of the cylinder defined in the initialization. The intersection of two lines in 3D space it is only possible if they lay on a common plane. Otherwise, the lines are skew and the shortest distance between them is established. The intersection point is defined in the middle of a line that is perpendicular to both intersected lines and whose length is the minimized distance.

With each estimated intersection point, a distance d_i between this point and the cylinder axis is determined. These distance values (cost-function) for all image points are afterwards minimized to adjust the parameters of the cylinder by means of iterative Best-fit methods.

The distance d_i between 2 spatial lines defined by each transformed point P_i (X_i, X_i, Z_i) and a characteristic point P_C (X_c, Y_c, Z_c) corresponding to the cylinder axis with their respective direction cosines n_i (a_i, b_i, c_i) and n_c (a_c, b_c, c_c) is determined by

$$d_i = \frac{\pm \begin{vmatrix} X_i - X_c & Y_i - Y_c & Z_i - Z_c \\ a_i & b_i & c_i \\ a_c & b_c & c_c \end{vmatrix}}{\sqrt{a^2 + b^2 + c^2}} \quad (12)$$
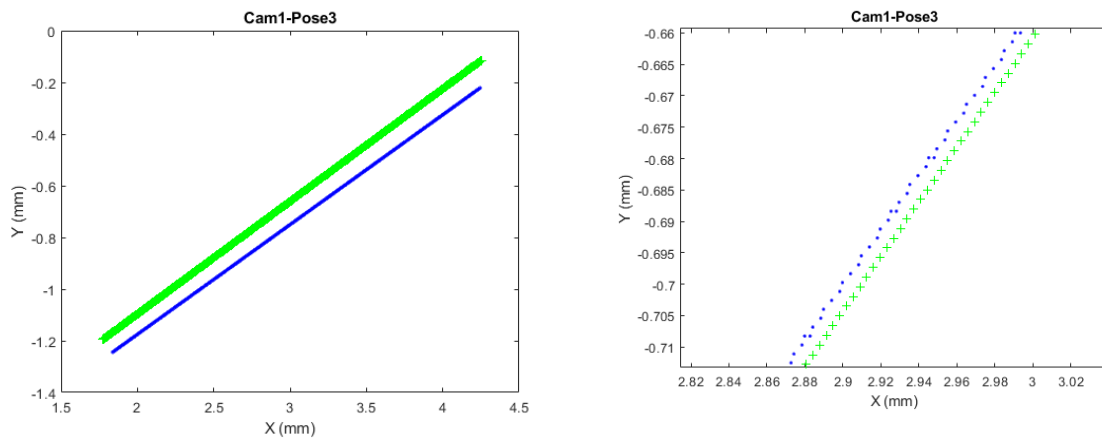
(a)
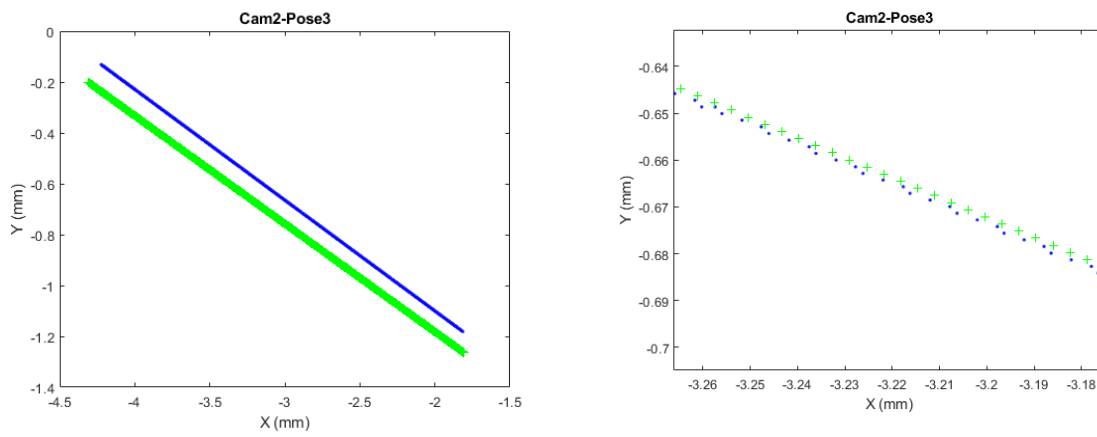
(b)
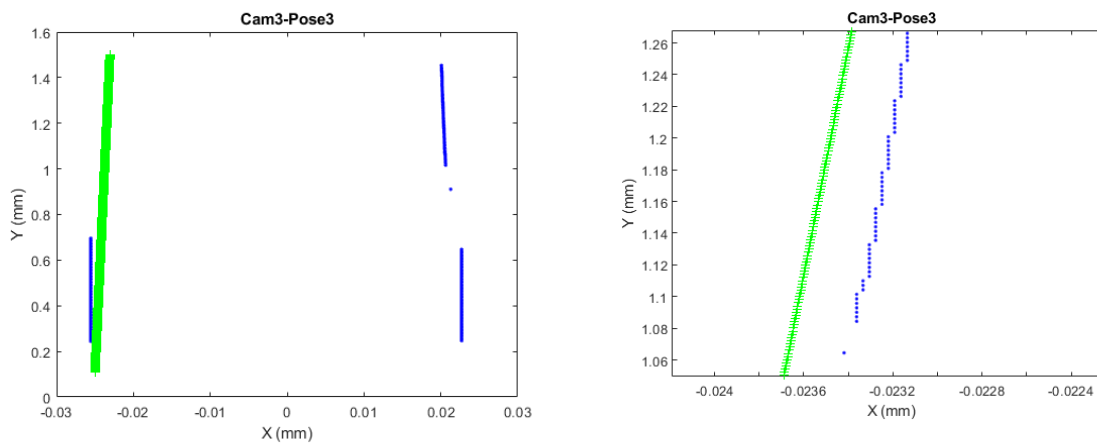
(c)

Figure 11. Qualitative comparison of reference (green) and synthetic (blue) image data for an oblique pose, each camera view and one side contour points. (a) Cam1-Pose3. (b) Cam2-Pose3. (c) Cam3-Pose3.

where,

$$a = \begin{vmatrix} a_i & b_i \\ a_c & b_c \end{vmatrix} \quad b = \begin{vmatrix} b_i & c_i \\ b_c & c_c \end{vmatrix} \quad c = \begin{vmatrix} c_i & a_i \\ c_c & a_c \end{vmatrix}. \quad (13)$$

The cylinder known radius (r) is subtracted to each estimated radial distance. The residual distance values among the image rays (3D lines) and the cylinder axis for all image points (i) and cameras (j) are minimized according to:

$$\sum_j \sum_i d_{ij}^2 - r = \min. \quad (14)$$

In order to solve this minimization problem, a linearization of the cost function is required for each parameter of the cylinder's model and each image point data which enables to construct the jacobian matrix (Kosmopoulos 2011, Afzal *et al* 2016, Hansen and Sutherland 2018) and estimate the corrections of model's parameters in each iteration. The convergence for the solver is obtained when the correction values (ΔP_c and Δn_c) of the element's geometric parameters are below a suitable threshold value.

The form of linearized equations follows

$$\frac{\partial d_{ij}}{\partial x} \cdot \Delta X_c + \frac{\partial d_{ij}}{\partial y} \cdot \Delta Y_c + \frac{\partial d_{ij}}{\partial z} \cdot \Delta Z_c$$
$$+ \frac{\partial d_{ij}}{\partial a} \cdot \Delta a_c + \frac{\partial d_{ij}}{\partial b} \cdot \Delta b_c + \frac{\partial d_{ij}}{\partial c} \cdot \Delta c_c = -d_{ij}. \quad (15)$$

The employed iterative method for minimization problem is not specified in detail as it is common issue in bibliographic references concerning inverse problems (Gao *et al* 2016, Nowak 2017, Ramm 2018) and it is out of the scope of this research.

2.3. Validation and testing

The validation of the implemented model is an important issue that ensures that the obtained results are accurate and meaningful, and therefore the conclusions in relation to these results can be considered truthful. For this purpose, a validated trigonometric approach was employed to check the partial data and results of the developed model. Once the model was approved, further tests were carried out to understand its scope concerning error sources and possible deviations between the theoretical model and the real scene. Moreover a Montecarlo simulation approach was established to estimate cylinder pose uncertainties and determine model's output distribution.

2.3.1. Validation of the developed model.

The implementation of the developed model has been checked against an inspection tool called Spatial Analyzer© (hereafter SA) based on the same cylinder pose and camera network definition. This is a 3D inspection software that enables to reproduce the described photogrammetric approaches (see figure 9) from the point of view of pure trigonometry which permits to carry out 2D data validation and accuracy comparison in section 3.1 avoiding the part of image generation

Table 1. Quality analysis and differences between reference image data and synthetic data for an oblique pose.

Camera ID	Nominal (SA) FE (mm)	Synthetic FE (mm)	2D distance (mm)
1	0	0.10	0.05
2	0	0.10	0.05
3	0	0.06	0.14

and data processing. Facing this objective, the SA interface is used to replicate the developed model in terms of camera network, cylinder pose definition and image ray composition from image planes towards tangential 3D points in the cylinder. Every data is referenced to the main world coordinate system.

The employed procedure and workflow for 3D scene definition and reference data extraction is the following one:

1. A cylinder is placed for a specific pose (position and orientation)
2. Local coordinate systems are defined corresponding to external camera orientation
3. Image planes are created in these coordinate systems
4. Projection centers are defined for each image plane
5. A plane is estimated that in tangential to the cylinder surface and passes through each projection center (3×)
6. Tangential points above the cylinder surface are estimated projecting the cylinder axis to previously created tangential planes
7. With each point and its corresponding projection center, 3D lines are created
8. The intersection of these lines with the image planes describes the image points

Thus, applying this methodology, reference data can be used to check the implemented model. Among this data, 3D tangential points and image points both in local and global coordinate system are obtained. The employed scaling factor to convert pixel points in image coordinates (metric values) is 2.8387.

2.3.2. Test for validation and comparison of results.

The following chapters describe the tests and the targeted results for each test considering several aspects and parameters of the model. A symmetric camera network is studied which guarantees data redundancy and a proper visualization of the cylinder from different point of views. Asymmetric camera networks are not included in this paper, but asymmetry appears on 3D tangential point distribution all around the cylinder. First, a comparison among image data points comparing the values obtained from synthetic images and SA data is presented. Then, the accuracy of the developed model is analyzed based on image data and its inaccuracies, taking theoretically known pose values as *a priori* data. The model's robustness is tested with a deviation range of priori pose data to understand the dependency of the model on *a priori* known data values.

Table 2. Nominal and measured point comparison for all cylinder and pose case studies (Errors and uncertainties in mm).

POSE ID	Point ID	CS 1[a]		CS 2		CS 3		CS 4		CS 5	
		E_{xyz}	U_{xyz}	E_{xyz}	U_{xyz}	E_{xyz}	U_{xyz}	E_{xyz}	U_{xyz}	E_{xyz}	U_{xyz}
1	P1	0.28	0.26	2.93	0.26	0.59	0.25	0.60	0.25	0.05	0.09
	P2	1.27	0.34	1.42	0.35	0.71	0.30	1.58	0.43	0.77	0.23
2	P1	10.43	4.57	7.53	4.09	12.47	4.29	11.08	4.38	9.27	3.48
	P2	13.11	5.57	9.35	4.61	14.92	5.10	12.21	4.65	13.47	5.38
3	P1	8.57	4.63	7.68	3.51	6.52	2.98	6.43	4.03	9.81	3.50
	P2	11.77	5.77	9.92	4.87	8.56	3.22	8.69	4.77	17.83	4.80

[a] Case studies: 1 ($L = 8000$ mm and $D = 250$ mm), 2 ($L = 8000$ mm and $D = 500$ mm), 3 ($L = 8000$ mm and $D = 1000$ mm), 4 ($L = 4000$ mm and $D = 250$ mm), 5 ($L = 16\,000$ mm and $D = 250$ mm).

2.3.2.1.Comparison of synthetic image data and geometric data. Based on reference data obtained from the SA tool, a comparison among data types was carried out to verify and understand the differences between synthetic transformed image data (see equation (3)) applied to photogrammetric models and pure trigonometric precise data. In this manner, the effect of image to metric data transformation can be assessed and quantified.

This comparison can be established at two different stages of the model related with different data types. For instance, 2D image points can be compared with their corresponding 3D tangential points, but in this paper only 2D data are compared. The comparison comprises a qualitative and quantitative comparison between image data (see equation (2)) obtained with several cameras in their local coordinates (2D metric data). In the following chapter, 3D data resulting from the geometrical fitting are assessed to analyze their accuracy.

2.3.2.2. Accuracy of cylinder pose estimation model. After comparing the developed model against the reference 2D data and validating its performance, the accuracy for model parameters is assessed. This analysis is carried out on three poses of the cylinder for the different case studies, together with their respective synthetic data obtained from the procedure described in the process workflow (see figure 2). The aim of this test is to estimate pointing errors of the model by comparing the estimated cylinder parameters and the nominal values. Instead of comparing the obtained values of position and orientation with their nominals, two extreme points (P_1, P_2) of the cylinder (see figure 10) have been defined for each pose simulation case. The aim is to make easier the understanding of the results. Considering that extrinsic orientation of the camera network is precisely known and fixed, residuals are taken as model accuracy indicators.

Apart from mean positioning errors between estimated and nominal cylinder poses, *XYZ* coordinate uncertainties have been calculated for each cylinder point (P1 and P2) in order to understand the reliability of these results. This has been implemented by a Montecarlo simulation approach which enables to add image data and principal distance variations to the model. In this manner, the theoretical data is fitted to a more realistic scenario. The employed simulation parameter values are the following ones: image noise (0.5 pixels) and

principal distance uncertainty ±10 pixels. The convergence threshold values for this uncertainty assessment have been settled to 1 mm (average of residual tangential distances).

Moreover, cylinder dimensions (length and diameter) have been changed for each cylinder pose to check if this variation affects models accuracy. Lengths of 4, 8, 16 metres and diameters of 250, 500, 1000 mm have been tested as representative case studies.

2.3.2.3. Robustness of cylinder pose estimation model. Besides testing the accuracy of the model, its robustness is also tested. One of the requirements of this photogrammetric model is that approximated pose values of the cylinder are necessary to initialize it. Considering that real applications do not assure that the real pose and the nominal one are close to each other, this effect has been simulated and quantified to determine the model's robustness.

In this case, testing procedure consists in introducing initial errors for known poses and camera network to check the robustness and performance of the model. Errors ranging from 1 mm to 1000 mm are applied to *a priori* cylinder parameters (points P_1 and P_2 as in accuracy testing) and the model's response is studied for a 1 mm convergence threshold (which is the maximum value of correction parameter values). These errors are applied separately on each position coordinate (*XYZ*) and then combined for both points' coordinates (P_1 and P_2). Within this test a 8 m and 250 mm diameter cylinder case study has been studied.

Another interesting characteristic from the point of view of the model's robustness, is the minimum amount of image data required and their distribution along the contour lines of the cylinder. This aspect was also analysed when establishing the need for image data quality. The relationship between the model's input data and output data (pose estimation) was studied for the following cases and compared against full 2D data for pose 2:

- Continuous data taking into consideration only the contour points of one side (See case study B in table 3)
- Reduction of continuous image data points from 25% to 75% (See case studies C, D and E in table 3)
- 1/3th of image data for each camera view without correspondence for the same cylinder area (See case study F in table 3)

3. Results

The following results show the capabilities of the developed modelling from the point of view of accuracy and robustness, which are critical aspects for its characterization for future implementations in real applications.

3.1. Comparison of synthetic image data and geometric data

In order to validate and compare the quality of the image data when working with synthetic images in relation to reference data (SA), figure 11 presents, a qualitative comparison of image points on the left side, together with a detailed zoom on the right side. The represented case study corresponds to an oblique pose (pose 3) for a 8 m length and 250 of diameter cylinder. The comparison shows that the data obtained from 3D and transformed into 2D with SA is continuous and straight for contour points (green points) while the employed synthetic data present some imperfections. Regarding to synthetic data transformed to metric data (see equation (2)), the distribution of the points is not straight and even equidistant deviations are found compared against reference data (see zoom in right side for figure 11). Thus, it is obvious that synthetic data are not perfect and present some deviations derived/resulting from the rendering step and the edge point extraction approaches.

In order to analyze the deviation range numerically, in table 1 the error (FE) of each image data type and the 2D distance among fitted lines is shown for an oblique pose and 3 camera views. While the error form for SA reprojected image data is 0, the values for the synthetic are not negligible. These deviations are the main error sources that are conditioning 3D pose estimation accuracy analyzed in section 3.2.

In summary, it can be stated that the synthetic image data generation process is correctly implemented in the model and the procedure is accurate up to 0.14 mm for image coordinates corresponding to an oblique pose, which is the most critical case.

Although there is no way to guarantee/assure perfection, a possibility that could improve synthetic data accuracy is to use better rendering methods for image generation step. Thus, this error needs to be taken into account for these simulation procedures. Error minimization could be achieved by processing the input image data before the model feeding and then fitting these data as accurate contour 2D lines, but this approach would also introduce a systematic error for 3D distances estimated with the model.

3.2. Accuracy analysis of the model

The accuracy of the model has been established for all mentioned case studies (see section 2.3.2.2) and cylinder poses. Based on synthetic images, the image processing step, added imaging error sources and the previously described photogrammetric model (see section 2.2.3), the poses and uncertainties of the cylinder are estimated. In order to facilitate the comparison
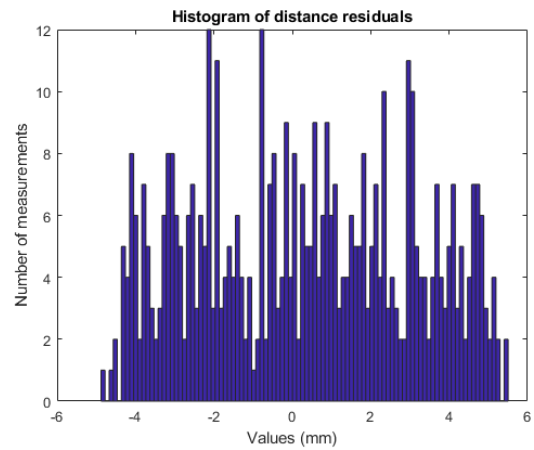
(a)
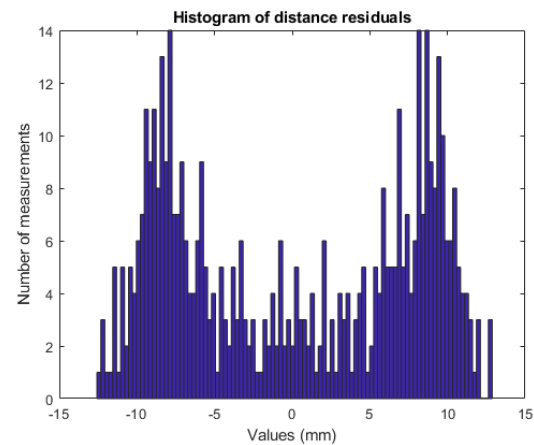
(b)
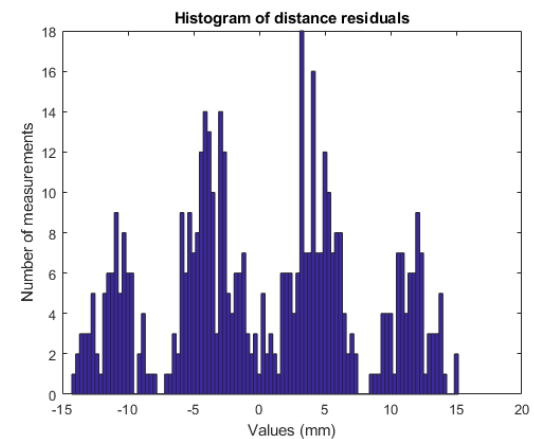
(c)

Figure 12. Histograms of distance residuals for estimated tangential points and cylinder axis for each nominal pose. (a) Pose1. (b) Pose2. (c) Pose3.

Table 3. Spatial positioning comparison for diverse 2D image data set. (A) Estimated values with both contour sides. (B) Estimated values with one contour side. (C) Estimate values with filtered contour points 25%. (D) Estimated values with filtered contour points 50%. (E) Estimated values with filtered contour points 75%. (F) Estimated values for not corresponding areas of the cylinder.

Case study ID	Point ID	Estimated coordinates (mm)			Differences (mm)		
		X	Y	Z	ΔX	ΔY	ΔZ
A	P1	−11 025.34	6355.53	−12 727.92	—	—	—
	P2	−6122.95	3529.23	−7072.95	—	—	—
B	P1	−11 018.88	6354.09	−12 727.92	6.46	1.44	0
	P2	−6126.19	3535.51	−7062.7	3.24	6.28	10.25
C	P1	−11 020.50	6353.43	−12 727.92	4.84	2.1	0
	P2	−6124.22	3535.31	−7063.59	1.27	6.08	9.36
D	P1	−11 019.48	6353.86	−12 727.92	5.86	1.67	0
	P2	−6124.72	3535.17	−7062.57	1.77	5.94	10.38
E	P1	−11 019.92	6353.95	−12 727.92	5.42	1.58	0
	P2	−6124.16	3535.12	−7063.49	1.21	5.89	9.46
F	P1	−11 009.31	6357.94	−12 727.92	16.03	2.41	0
	P2	−6139.51	3538.72	−7041.35	16.56	9.49	31.6

between obtained results and the nominal values, the pose is defined by means of two points (P1 and P2) that lay on the cylinder's axis and determine its length. This comparison is shown in table 2, where positioning errors (E_{xyz}) among nominal points and measured ones are presented as well as their uncertainty (U_{xyz}). For all the error values the mean differences are below 20 mm for working distances of 20 000 mm in radius (camera location) with uncertainties below ±5 mm. Therefore, the relative accuracy lays between 1/1000 and 1/20 000 for all case studies. Accuracy depends on the cylinder's pose and the image data quality mentioned in section 3.1, where deviations of tens of microns correspond to mm in 3D space due to projections effects. Moreover imaging error sources such as image noise and principal distance uncertainty add more error variability to image points. The more vertical the pose, the better results (ten times better for Pose1), because the contour points of the cylinder will be more accurately defined and detected. Although other rendering approaches were also employed for synthetic image generation, the results are similar, so the accuracy of the model is limited to this error source.

Besides, figure 12 presents a histogram for each pose, showing the residuals of the distances between the cylinder axis and the estimated 3D tangential points (see equation (12)) for case study1. As this figure shows, the residuals are not symmetric, and the differences tend to create groups which means that systematic errors are conditioning the results. This tendency is probably related to the deviations and the distribution of the image data points employed.

Although the range of the distance residual values for each pose corresponds to even tens of mm, the average values are similar to the absolute deviations of the points P1 and P2 analyzed in table 1.

3.3. Robustness analysis of the model

One aspect and limitation of the photogrammetric model is the need to know *a priori* data close to cylinder's pose. However, this requirement is not always assured with enough

accuracy, therefore, it is important to establish the robustness of the model regarding this aspect. Aiming at this, the model has been tested with *a priori* pose data with known *XYZ* deviations for P1 and P2 points and the fitting result was assessed. The expected result is the nominal pose correcting these initial deviations. After testing, the model for oblique and vertical poses for all case studies, the following can be stated:

- For *XY* position deviations, the residuals of points that define the cylinder pose are less than 1 mm for large working distances.
- For *Z* deviations, the model converges but the result is not robust because a reference along the axis is missing.
- Robustness does not depend on the cylinder pose; deviations are similar in both cases.
- The model depends on *a priori* pose knowledge, but the real position can deviate even few meters from supposed known values.

In order to analyze the image data effect on the cylinder pose fitting result, several cases were assessed changing both the number of points and its distribution along the contour points of the cylinder. As an example of this evaluation, table 3 presents the results for the cases presented in section 2.3.2.3 for the camera pose number 2 and cylinder dimensions of CS1. These tables present point coordinates P1 and P2, and the differences between them can be established taking them as a reference for case study A.

For any of the cases presented, the differences among each approach are not higher than 10 mm, except for the case where the image points for each camera view are not correspondent (See case study *F*). For this exception, the deviations for both *XY* and *Z* directions are higher because of a worse conditioned image data point distribution.

4. Discussion and conclusions

Results highlight that the theoretical model is suitable for close-range photogrammetric pose estimation and sensible

to *a priori* known data and image data quality. Therefore, it could be used with design purposes in order to fulfill measuring system requirements and select a suitable and affordable approach. In this research a symmetric camera network has been employed considering that is a rather realistic approach for real implementation. Other effects such as receiver deformation, camera network instabilities or computational efficiencies are not taken into account in this research. However, real scenery image data quality and disturbances due to high energy concentration effects as well as imaging parameter uncertainties are considered in the simulation process. The real materialization of the simulated photogrammetric approach will consider intrinsic and extrinsic calibration methods, referencing methods and cylinder pose estimation testing against certified measuring procedures. Thus experimental tests will be carried out once the overall procedure is established and every tool is prepared. The obtained results will be correlated with the model's performance.

With these preliminary results, it can be concluded that the model is accurate, and that this simulation procedure enables the obtaining of cylinder pose values with relative low deviations so that the suitability of tracking application requirements can be assessed. The relative accuracy of the model falls between 1/1000 and 1/20 000 with uncertainties of ± 5 mm for all case studies and poses. In the future, further synthetic data generation procedures and tools will be studied to speed up the simulation procedure and steps as they are time-consuming tasks.

The model is conditioned to initial *a priori* pose values that are not always known or provided, so it would be preferable to improve the independency of the model in this sense. Nevertheless, in some applications this fact does not constitute a limitation. For example, in a positioning control loop, the position previous to the one that is to be estimated is always known and it is very similar.

The robustness of the model is strong for the cylinder's axis orientation but weaker for spatial position determination. In order to improve this functionality and therefore, the response of the model, a model-based 3D circle estimation approach is required so as to combine it with the procedure presented in this paper. Higher model performance for five dof accurate pose estimation could be achieved with a combination of both approaches

According to the image data point number and distribution, it has been demonstrated that the model is robust when the image data is well distributed along the cylinder. Besides, in order to improve the computation time of the model, high data filtering is possible, thus assuring the same accuracy level.

Acknowledgments

Author contributions

EG-A designed the 3D scene poses in SW© and created the synthetic images, JM processed the images and created the data files, GK developed the photogrammetric model and simulated its capabilities, AT and RM reviewed the overall concept, GK also wrote the paper and all co-authors checked it considering their contribution and expertise.

Conflicts of interest

The authors declare no conflict of interest.

ORCID iDs

Gorka Kortaberria ⬤ https://orcid.org/0000-0001-9487-7425

References

Andresen K and Qifeng Yu 1994 Calculation of the geometric parameters of an ellipse in space by its edges in the images *ISPRS J. Photogramm. Remote Sens.* **49** 33–7

Afzal M, Arteaga I L and Kari L 2016 An analytical calculation of the Jacobian matrix for 3D friction contact model applied to turbine blade shroud contact *Comput. Struct.* **177** 204–17

Alsadik B S, Gerke M and Vosselman G 2012 Optimal camera network design for 3D modeling of cultural heritage *ISPRS Ann. Photogramm. Remote Sens. Spatial Inf. Sci.* **I-3** 7–12

Becke M and Schlegl T 2015 Least squares pose estimation of cylinder axes from multiple views using contour line features *IECON 2015—41st Annual Conf. of the IEEE Industrial Electronics Society* vol 3 pp 1855–61

Becke M 2015 On modeling and least squares fitting of cylinders from single and multiple views using contour line features, Eds H Liu, N Kubota, X Zhu, R Dillmann and D Zhou *Intelligent Robotics and Applications*: ICIRA 2015 vol 9246 (Cham: Springer) pp 812–23

Becker T A, Özkul M A and Stilla U B 2011 Simulation of close-range photogrammetric systems for industrial surface inspection *Int. Arch. Photogramm. Remote Sens. Spatial Inf. Sci.* **38** 179–83

Buffa F, Pinna A and Sanna G 2016 A simulation tool assisting the design of a close range photogrammetry system for the sardinia radio telescope *ISPRS Ann. Photogramm. Remote Sens. Spatial Inf. Sci.* **III-5** 113–20

Crc C F 2015 Advances in close-range photogrammetry Prof. Clive Fraser Evolution 1: Film to Digital Evolution 2: Manual to Automatic Image Meas. and Orientation Evolution 3: Manual Feature Extraction and Graphical Output to Automatic 3D Point Cloud Generation pp 7–11

Dall'Asta E, Thoeni K, Santise M, Forlani G, Giacomini A and Roncella R 2015 Network design and quality checks in automatic orientation of close-range photogrammetric blocks *Sensors* **15** 7985–8008

Doignon C 2007 An Introduction to model-based pose estimation and 3D tracking techniques *Reconstruction, Pose Estimation and Tracking* ed Rustam Stolkin (Vienna: I-Tech) pp 1–530

Doignon C and De Mathelin M 2007 A degenerate conic-based method for a direct fitting and 3D pose of cylinders with a single perspective view *Proc. IEEE Int. Conf. on Robotics and Automation* pp 4220–5

Dunn E 2007 Development of a practical photogrammetric network design using evolutionary computing *Photogramm. Rec.* **22** 22–38

El-hamrawy S, El-din Fawzy H and Al-Tobgy M 2016 Optimum design for close range photogrammetry network using particle swarm optimization technique *IOSR J. Mech. Civ. Eng.* **13** 17–23

Ferri M, Mangili F and Viano G 1993 Projective pose estimation of linear and quadratic primitives in monocular computer vision *CVGIP Image Underst.* **58** 66–84

Figueiredo R, Moreno P and Bernardino A 2017 Robust cylinder detection and pose estimation using 3D point cloud information *IEEE Int. Conf. on Autonomous Robot Systems and Competitions* pp 234–9

Fraser C, Jazayeri I and Cronk S 2010 A feature-based matching strategy for automated 3D model reconstruction in multi-image close-range photogrammetry *American Society for Photogrammetry and Remote Sensing Annual Conf. 2010: Opportunities for Emerging Geospatial Technologies* vol 1 pp 175–83 (www.scopus.com/inward/record.uri?eid=2-s2.0-84868587896&partnerID=40&md5=3dc2d82cad7d24d8dce587cd23e2798f)

Fraser C and Stamatopoulos C 2014 Automated target-free camera calibration *Proc. of the ASPRS 2014 Annual Conf.* vol II-5 (https://doi.org/10.5194/isprsannals-II-5-339-2014)

Fraser C S 2013 Automatic camera calibration in close range photogrammetry *Photogramm. Eng. Remote Sens.* **79** 381–8

Gao W, Leng J and Zhou X 2016 Iterative minimization algorithm for efficient calculations of transition states *J. Comput. Phys.* **309** 69–87

Guo X, Chen Y, Wang C, Cheng M, Wen C and Yu J 2016 Automatic shape-based target extraction for close-range photogrammetry *Int. Arch. Photogramm. Remote Sens. Spatial Inf. Sci.* **XLI-B1** 583–7

Gruen A and Li H 1991 Extraction of 3D linear features from multiple images by LSB-snakes *Proc. SPIE* **3072** 119–30

Hafez A Z, Soliman A, El-metwally K A and Ismail I M 2017 Design analysis factors and specifications of solar dish technologies for different systems and applications *Renew. Sustain. Energy Rev.* **67** 1019–36

Hanekr R, Navabi N and Appelt M 1999 Yet another method *Proc. 1999 IEEE Computer Society Conf. on Computer Vision and Pattern Recognition* vol 2 pp 544–50

Hansen M A and Sutherland J C 2018 On the consistency of state vectors and Jacobian matrices *Combust. Flame* **193** 257–71

Harun M H and Sulaiman M 2011 Shape-based matching : application of edge detection using Harris point shape-based matching: application of edge detection using Harris point *Int. Conf. Robot. Autom. Syst.* (https://doi.org/10.13140/RG.2.1.2151.2808)

Heipke C, Madden M, Li Z and Dowman I 2016 Theme issue 'state-of-the-art in photogrammetry, remote sensing and spatial information science' *ISPRS J. Photogramm. Remote Sens.* **115** 1–2

Hilton A 2005 Scene modelling from sparse 3D data *Image Vis. Comput.* **23** 900–20

Houqin B and Jianbo S 2008 Feature matching based on geometric constraints in weakly calibrated stereo views of curved scenes *J. Syst. Eng. Electron.* **19** 562–70

Huang J B, Chen Z and Chia T L 1996 Pose determination of a cylinder using reprojection transformation *Pattern Recognit. Lett.* **17** 1089–99

Joon Ahn S and Rauh W 2001 Circular coded target for automation of optical 3D—Measurement and camera calibration *Int. J. Pattern Recognit. Artif. Intell.* **15** 905–19

King P, Comley P and Sansom C 2013 Parabolic trough surface form mapping using photogrammetry and its validation with a large coordinate measuring machine *Energy Procedia* **49** 118–25

Knyaz V A 1998 Non contact 3D model reconstruction using coded targets *Int. Conf. Graphicon*

Kosmopoulos D I 2011 Robust Jacobian matrix estimation for image-based visual servoing *Robot. Comput.-Integr. Manuf.* **27** 82–7

Lee C D, Huang H C and Yeh H Y 2013 The development of sun-tracking system using image processing *Sensors* **13** 5448–59

Liu C and Hu W 2014 Relative pose estimation for cylinder-shaped spacecrafts using single image *IEEE Trans. Aerosp. Electron. Syst.* **50** 3036–56

Liu Y J, Zhang J B, Hou J C, Ren J C and Tang W Q 2013 Cylinder detection in large-scale point cloud of pipeline plant *IEEE Trans. Vis. Comput. Graphics* **19** 1700–7

Luhmann T 2016 Learning photogrammetry with interactive software Tool PhoX *Int. Arch. Photogramm. Remote Sens. Spatial Inf. Sci.* **41** 39–44

Luhmann T, Fraser C and Maas H G 2016 Sensor modelling and camera calibration for close-range photogrammetry *ISPRS J. Photogramm. Remote Sens.* **115** 37–46

Luhmann T, Robson S, Kyle S and Boehm J 2013 *Close-Range Photogrammetry and 3D Imaging. Close-Range Photogrammetry and 3D Imaging* 2nd edn (Berlin: De Gruyter) (https://doi.org/10.1515/9783110302783)

Luhmann T, Robson S, Kyle S and Harley I 2006 *Close Range Photogrammetry: Principles, Methods and Applications. LibTuDelftC* 1st edn (Dunbeath: Whittles Publishing)

Navab N and Appel M 2006 Canonical representation and multi-view geometry of cylinders *Int. J. Comput. Vis.* **70** 133–49

Nowak I 2017 Bayesian approach applied for thermoacoustic inverse problem *Energy* **141** 2519–27

Oberkampf D, DeMenthon D F and Davis L S 1996 Iterative pose estimation using coplanar feature points *Comput. Vis. Image Underst.* **63** 495–511

Olague G and Mohr R 2002 Optimal camera placement for accurate reconstruction *Pattern Recognit.* **35** 927–44

Osada R, Funkhouser T, Chazelle B and Dobkin D 2001 Matching 3D models with shape distribution *Shape Modeling and Applications, SMI 2001 Int. Conf.* pp 154–66

Paláncz B, Awange J L, Somogyi A, Rehány N, Lovas T, Molnár B and Fukuda Y 2016 A robust cylindrical fitting to point cloud data *Aust. J. Earth Sci.* **63** 665–73

Pappa R S, Giersch L R and Quagliaroli J M 2001 Photogrammetry of a 5 m inflatable space antenna with consumer-grade digital cameras *Exp. Tech.* **25** 21–9

Penman D W and Alwesh N S 2006 3D pose estimation of symmetrical objects of unknown shape *Image Vis. Comput.* **24** 447–54

Piatti E J and Lerma J L 2013 Virtual worlds for photogrammetric image-based simulation and learning *Photogramm. Rec.* **28** 27–42

Pottler K, Lüpfert E, Johnston G H G and Shortis M R 2005 Photogrammetry: a powerful tool for geometric analysis of solar concentrators and their components *J. Sol. Energy Eng.* **127** 94

Puech W, Chassery J-M and Pitas I 1997 Cylindrical surface localization in monocular vision vol 18 pp 711–22

Rabbani T and Van Den Heuvel F 2005 Efficient hough transform for automatic detection of cylinders in point clouds *ISPRS Workshop on Laser Scanning* vol 3 pp 60–5

Ramm A G 2018 Inverse problem of potential theory *Appl. Math. Lett.* **77** 1–5

Renaud P, Andreff N, Philippe M and Gogu G 2005 Kinematic calibration of parallel mechanisms: a novel approach using legs observation *IEEE Trans. Robot.* **21** 529–38

Rosenhahn B, Brox T, Cremers D and Seidel H P 2006 A comparison of shape matching methods for contour based pose estimation *Lecture Notes in Computer Science* (*Including Subseries Lecture Notes in Artificial Intelligence and Lecture Notes in Bioinformatics* vol 4040) (LNCS) Eds R Reulke *et al* (Berlin: Springer) pp 263–76

Ruelas A, Velázquez N, Villa-Angulo C, Acuña A, Rosales P and Suastegui J 2017 A solar position sensor based on image vision *Sensors* **17** 1–13

Shiu Y C and Huang C 1991a Pose determination of circular cylinders using elliptical aiid side projections pp 265–8

Shiu Y C and Huang C 1991b Locating cylindrical objects from perspective projections *Proc. of the IEEE 1991 National Aerospace and Electronics Conf. NAECON 1991* (https://doi.org/10.1109/NAECON.1991.165892)

Shortis M R and Johnston G H G 1996 Photogrammetry: an available surface characterization tool for solar concentrators, {P}art {I}: measurement of surface *J. Sol. Energy Eng.* **118** 146–50

Shortis M R, Johnston G H G, Pottler K, Lüpfert E and Commission V 2008 Photogrammetric analysis of solar collectors *Int. Arch. Photogramm. Remote Sens. Spatial Inf. Sci.* **37** 81–8

Shortis M R, Seager J W, Robson S and Harvey E S 2004 Automatic recognition of coded targets based on a hough transform and segment matching *Electronic Imaging. Videometrics VII* p 5013

Stynes J K and Ihas B 2012 Slope error measurement tool for solar parabolic trough collectors preprint Pix 16560 (https://doi.org/10.1115/1.3035811)

Su Y-T and Bethel J 2010 Detection and robust estimation of cylinder features in point clouds *ASPRS* vol 2, pp 887–93

Summan R, Pierce S G, Macleod C N, Dobie G, Gears T, Lester W, Pritchett P and Smyth P 2015 Spatial calibration of large volume photogrammetry based metrology systems *Measurement* **68** 189–200

Teck L W, Sulaiman M, Shah H N M and Omar R 2010 Implementation of shape—based matching vision system in flexible manufacturing system *J. Eng. Sci. Technol. Rev.* **3** 128–35

Teney D and Piater J 2014 Multiview feature distributions for object detection and continuous pose estimation *Comput. Vis. Image Understand.* **125** 265–82

Triggs B 1999 Camera pose and calibration from 4 or 5 known 3D points *Proc. of the 7th IEEE Int. Conf. on Computer Vision* vol 1 pp 278–84

Tushev S and Sukhovilov B 2017 Photogrammetric system accuracy estimation by simulation modelling *2017 Int. Conf. on Industrial Engineering, Applications and Manufacturing (ICIEAM)* pp 1–6

Veldhuis H and Vosselman G 1998 The 3D reconstruction of straight and curved pipes using digital line photogrammetry *ISPRS J. Photogramm. Remote Sens.* **53** 6–16

Wijenayake U, Choi S I and Park S Y 2014 Automatic detection and decoding of photogrammetric coded targets *13th Int. Conf. on Electronics, Information, and Communication, ICEIC 2014—Proc.* pp 1–2

Xu S and Liu M 2013 Feature selection and pose estimation from known planar objects using monocular vision *2013 IEEE Int. Conf. on Robotics and Biomimetics (ROBIO)* pp 922–7

Yang C, Feinen C, Tiebe O, Shirahama K and Grzegorzek M 2016 Shape-based object matching using interesting points and high-order graphs *Pattern Recognit. Lett.* **83** 251–60

Zhang T, Liu J, Liu S, Tang C and Jin P 2017 A 3D reconstruction method for pipeline inspection based on multi-vision *Measurement* **98** 35–48

Zhi L and Tang J 2002 A complete linear 4-point algorithm for camera pose determination *AMSS Acad. Sin.* **21** 239–49

Zhu Z, Stamatopoulos C and Fraser C S 2015 Accurate and occlusion-robust multi-view stereo *ISPRS J. Photogramm. Remote Sens.* **109** 47–61